19. Demidov V A *IEEE Trans. Plasma Sci.* **38** 1773 (2010)
20. Pavlovskii A I et al., Invention Certificate No. 243103. MKI H02N 11/00. Priority of 28.22.67; *Byull. Izobret.* (33) (1969)
21. Veselov V N et al., Invention Certificate No. 1409087. MKI H02N 11/00. Priority of 09.10.85; *Byull. Izobret.* (13) (2000)
22. Demidov V A *IEEE Trans. Plasma Sci.* **38** 1780 (2010)
23. Selemir V D et al., in *Megagaussnaya i Megaampernaya Impul'snaya Tekhnologiya i Primenenie* (Megagauss and Megaampere Pulsed Technology and Applications) (Eds V K Chernyshev, V D Selemir, L N Plyashkevich) (Sarov: RFYaTs – VNIIEF, 1997) p. 248
24. Chernyshev V K, Volkov G I, Vakhrushev V V, in *Megagauss Physics and Technology* (Ed. P J Turchi) (New York: Plenum Press, 1980) p. 663
25. Pavlovskii A I, Vasyukov V A, Russkov A S *Pis'ma Zh. Tekh. Fiz.* **3** 789 (1977)
26. Petrukhin A A et al., in *Sverkhsil'nye Magnitnye Polya. Fizika. Tekhnika. Primenenie* (Superhigh Magnetic Fields. Physics. Technology. Applications) (Eds V M Titov, G A Shvetsov) (Moscow: Nauka, 1984) p. 384
27. Chernyshev V K et al., in *Megagauss Field and Pulsed Power Systems* (Eds V M Titov, G A Shvetsov) (New York: Nova Sci. Publ., 1990) p. 465
28. Demidov V A, Skokov V I, in *Megagaussnaya i Megaampernaya Impul'snaya Tekhnologiya i Primenenie* (Megagauss and Megaampere Pulsed Technology and Applications) (Eds V K Chernyshev, V D Selemir, L N Plyashkevich) (Sarov: RFYaTs – VNIIEF, 1997) p. 385
29. Petrukhin A A et al., in *Sverkhsil'nye Magnitnye Polya. Fizika. Tekhnika. Primenenie* (Superhigh Magnetic Fields. Physics. Technology. Applications) (Eds V M Titov, G A Shvetsov) (Moscow: Nauka, 1984) p. 406
30. Chernyshev V K et al., in *Megagauss Field and Pulsed Power Systems* (Eds V M Titov, G A Shvetsov) (New York: Nova Sci. Publ., 1990) p. 533
31. Chernyshev V K et al., in *Megagauss Magnetic Field Generation and Pulsed Power Applications* (Eds V Cowan, R B Spielman) (New York: Nova Sci. Publ., 1994) p. 731
32. Demidov V A et al. *IEEE Trans. Plasma Sci.* **38** 1768 (2010)
33. Chernyshev V K et al., in *Megagauss Magnetic Field Generation and Pulsed Power Applications* (Eds V Cowan, R B Spielman) (New York: Nova Sci. Publ., 1994) p. 519
34. Buiko A M et al. *Vopr. At. Nauki Tekh. Metod. Prog. Chisl. Resh. Zadach Mat. Fiz.* (3(14)) 30 (1983)
35. Buiko A M et al. *Dokl. Akad. Nauk SSSR* **344** 323 (1992)
36. Veselov V N et al., Invention Certificate No. 1616386. MKI H02N 11/00. Priority of 14.03.88; *Byull. Izobret.* (22) (1995)
37. Demidov V A et al., Invention Certificate No. 1526480. MKI H02N 11/00. Priority of 14.03.88; *Byull. Izobret.* (6) (1996)
38. Demidov V A, Kazakov S A *IEEE Trans. Plasma Sci.* **38** 1758 (2010)
39. Selemir V D, Demidov V A, Repin P B *IEEE Trans. Plasma Sci.* **38** 1754 (2010)
40. Brodskii A Ya et al. *Dokl. Akad. Nauk SSSR* **314** 846 (1990) [*Sov. Phys. Dokl.* **35** 876 (1990)]
41. Vasyukov V A et al., in *Proc. of the 13th Intern. Conf. on Megagauss Magnetic Field Generation and Related Topics, 2010* (to be published)
42. Pavlovskii A I et al., in *Megagauss Magnetic Field Generation and Pulsed Power Applications* (Eds V Cowan, R B Spielman) (New York: Nova Sci. Publ., 1994) p. 969
43. Pavlovskii A I et al., in *Megagauss Magnetic Field Generation and Pulsed Power Applications* (Eds V Cowan, R B Spielman) (New York: Nova Sci. Publ., 1994) p. 977
44. Selemir V D et al., in *Proc. of the 15th IEEE Intern. Pulsed Power Conf., Monterey, Calif., 2005* (Eds J Maenchen, E Schamiloglu) p. 541
45. Arinin V A et al., in *Megagauss Magnetic Field Generation and Related Topics, Berlin, Germany, 2005* (Ed. M Von Ortenberg) p. 348
46. Spielman R B et al., in *Proc. of the 10th IEEE Intern. Pulsed Power Conf., Albuquerque, NM, USA, 1995* (Eds W Baker, G Cooperstein) p. 396
47. Dyabilin K S et al. *Teplofiz. Vys. Temp.* **34** 479 (1996) [*High Temp.* **34** 473 (1996)]
48. Selemir V D et al. *Fiz. Plazmy* **25** 1085 (1999) [*Plasma Phys. Rep.* **25** 1000 (1999)]
49. Selemir V D et al. *Fiz. Plazmy* **33** 424 (2007) [*Plasma Phys. Rep.* **33** 381 (2007)]
50. Ivanovsky A V et al., in *VIII Kharitonovskie Chteniya po Problemam Fiziki Vysokikh Plotnostei Energii* (VIIIth Khariton Readings on the Problems of High Energy Density Physics) (Sarov: RFYaTs – VNIIEF, 2006) p. 563
51. Dolgachev G I et al. *Prib. Tekh. Eksp.* (2) 1 (2007)

PACS numbers: **07.35.+k**, **47.40.–x**, 61.05.C–
DOI: 10.3367/UFNe.0181.201104l.0427

Pulsed X-ray diffraction structure study of shocked materials

A M Podurets

Shock wave investigations are performed, as a rule, by measuring physical quantities which provide only indirect information on the structure of matter behind the shock wave (SW) front. Thus, the structure of high-pressure phases is mainly obtained from experiments on the static compression or laboratory studies of samples preserved after shock loading. At the same time, it is obvious that no direct correspondence between structures in static and dynamic experiments can exist because of the difference in the time scales of processes proceeding in these experiments. Therefore, the problem of obtaining structural information directly in shock wave experiments becomes very important. In addition, the equations of state are studied, as a rule, by interpreting the SW data based on the assumption of the complete relaxation of materials (the hydrodynamic approximation); however, this assumption should also be verified. The only direct method for studying the structure of materials immediately behind the SW front is pulsed X-ray diffraction (PXRD) analysis. This method attracts great interest because it provides X-ray patterns of a substance recorded during its compression by a SW, i.e. for no more that a few hundred nanoseconds.

The aim of this paper is to review the results of PXRD studies obtained for more than 40 years of applying this method. The review is based on work performed at the Russian Federal Nuclear Center — All-Russian Research Institute of Experimental Physics (ARIEP or VNIIEF in *Russ. abbr.*).

In the second half of the 1960s, L V Al'tshuler, L A Egorov and their coauthors developed and demonstrated a technique for photographing structural X-ray patterns during times on the order of 1 μs [1, 2]. Soon, the problem of recording pulsed X-ray patterns at the moment of action of shock waves on a sample was also solved [3].

The X-ray diffraction analysis is based on the linkage between the X-ray scattering angle θ and the spacing d of

A M Podurets Federal State Unitary Enterprise 'Russian Federal Nuclear Center — All-Russian Research Institute of Experimental Physics', Sarov, Nizhny Novgorod region, Russian Federation
E-mail: am.podurets@gmail.com

Uspekhi Fizicheskikh Nauk **181** (4) 427 – 434 (2011)
DOI: 10.3367/UFNr.0181.201104l.0427
Translated by M Sapozhnikov; edited by A Radzig

crystal lattice planes described by the Bragg relation

$$2d\sin\theta = \lambda\,,$$

where λ is the radiation wavelength (the method is used in the range where λ and d are of the same order of magnitude). Thus, a change in the crystal structure (d) is determined by a change in the angular position of a diffraction line (by its 'shift').

The two basic problems to be solved by researchers using this method were:

(1) How is a crystal lattice deformed behind the SW front?

(2) What is a material structure in the case of its phase transformation in the SW? (This is especially interesting if the high-pressure phase is not recovered after unloading to the normal pressure, thereby becoming inaccessible for structural studies by standard materials science methods.)

The first PXRD studies were published at the early 1970s by Soviet [3] and American [4–6] researchers. Soon, similar studies were also performed in France [7], Japan [8–11], and Germany [12].

The arrangement of PXRD experiments involve a number of difficulties. The first of them is the proper selection of samples for analysis. The required exposure times are short, and therefore only samples with a high reflectivity can be used. This imposes restrictions on both the sample material and its structure. In most papers, the single crystals of LiF, NaCl, KCl, SiO_2, Si, Bi, and some other materials were investigated. This is explained by the fact that single crystals, being in a proper reflecting position, give considerably more intense reflections in X-ray patterns than polycrystalline materials (a single crystal as a whole reflects radiation in one direction, whereas in a polycrystal only a part of the grains with a certain orientation are involved in radiation reflection). However, the photography of polycrystals (when possible) offers some advantages; in particular, it is possible to obtain at once several reflections in one X-ray pattern by using monochromatic radiation. Sometimes it is possible to record a rather intense X-ray pattern by utilizing polycrystals with a pronounced texture.

The method was further developed and X-ray pattern photography schemes were proposed to obtain simultaneously two reflections from the two planes of a single crystal in one experiment [13]. This method, which is called multiple X-ray diffraction [14, 15], allows one to investigate the compressibility of crystals in two mutually perpendicular directions under the same loading conditions and even in one experiment.

The intensity of a diffraction line (neglecting the crystal structure type) is defined as

$$I \sim \frac{1}{\mu\rho}\,,$$

where μ is the mass radiation absorption coefficient of a sample material, and ρ is the density. Therefore, samples consisting of elements with small atomic numbers are, as a rule, preferable for studies because the X-ray absorption coefficient μ increases with increasing atomic number and, hence, the amount of material involved in the formation of reflections decreases.

Another important problem in experiments is the synchronization of a radiation source with a device generating SWs in the sample. The lifetimes of the states in SW-loaded samples rarely exceed a few fractions of a microsecond. Correspondingly, the PXRD exposure times are from about 0.1–1 ns (upon excitation of an X-ray pulse by a laser beam) [16, 17] up to approximately 100–200 ns when pulsed X-ray tubes are used [3, 8].

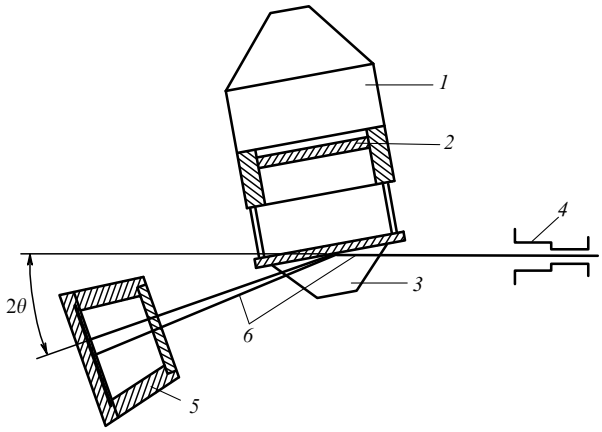

Figure 1. Schematic of the experimental setup [3]: (*1*) explosive charge; (*2*) accelerated striker; (*3*) lithium layer; (*4*) X-ray collimator; (*5*) X-ray film holder, and (*6*) incident and reflected beams.

Upon excitation of SWs in a sample, the equipment (the detection system and radiation source) can be damaged by explosion fragments or products. Therefore, it is necessary to protect the equipment, including detectors, during experiments from the possible action of an SW generator. Below, we will consider some options for organizing experiments and their peculiarities.

Figure 1 displays the layout of related experiments performed at VNIIEF [3, 18, 19]. A generally similar scheme was also employed in the work of other researchers. The mutual geometrical arrangement of a pulsed X-ray source, a sample, and a radiation detector corresponds to the focusing of X-rays (it can be different in various experimental setups).

The general focusing condition in experiments with flat samples is expressed by the Kurdyumov relation [20]

$$\tan\psi = \frac{\sin 2\theta}{\cos 2\theta + L/l}\,,$$

where ψ is the angle between the incident beam and a sample, θ is the diffraction angle, and L and l are the distances from the sample to the radiation source and detector, respectively. The relation between L and l is chosen to avoid damage to the detector and source, providing the required X-ray pattern intensity.

The sample is loaded with a plane SW produced by a striker which is accelerated by the explosion of a chemical explosive. This method was used in most work performed at VNIIEF and in the work of Q Johnson and coauthors [5, 6]. Shock waves can also be produced by using an electric explosion [12, 21, 22] or a solid propellant [7, 23] or gas [8, 9, 24, 25] gun. In Refs [16, 17, 26], SWs were generated in silicon samples by a laser pulse. The range of pressures achieved in experiments depends on the method of generating sample-loading SWs. Thus, pressures achieved in samples (up to a few GPa) by using an electric explosion or a powder accelerator are lower than those obtained in experiments with explosives or gas guns (up to a few dozen GPa). The diagnostics of the gas-dynamic characteristics in laser-loading experiments was

poorly developed and therefore the pressures achieved in these experiments could be estimated only approximately or obtained from calculations. Another significant advantage of explosives and guns is the possibility of keeping a sample under pressure for some time (in the presence of a stationary loading wave).

X-ray patterns are usually photographed through a supporting layer of a light inert material preventing the sample from unloading during measurements. This layer, which is simultaneously transparent to X-rays, can be made of lithium, carbon, beryllium, or Plexiglas. By photographing without the supporting layer, it is possible to detect the state existing in the sample immediately after its unloading. In this way, information on the stability of the high-pressure phase in a rarefaction wave can be obtained [27].

We used in our experiments pulsed X-ray tubes of various designs with a copper or a molybdenum anode. The diffracted radiation was detected with an X-ray film or photosensitive equipment.

To interpret X-ray diffraction patterns obtained in experiments, it is necessary to relate the observed reflections to the absolute scale of diffraction angles. The simplest solution to this problem reduces to X-ray photographing a sample in the same geometry before and during the SW action. In this case, the angular position of lines in the explosion X-ray pattern is determined by their displacement with respect to the lines of the unloaded sample in a preliminary photograph. Sometimes it is possible to obtain simultaneously the photographs of the uncompressed and compressed structure on the same film. In this regard, synchronization is performed so that a part of the exposure falls at the uncompressed state before the SW arrival, while another part falls at the already compressed state [9]. A similar effect can also be achieved by photographing a thin compressed layer, when the yet uncompressed crystal layer lying under the former is also simultaneously 'seen' [17]. Photographing samples by utilizing standard samples is also applied. As a standard, a material can be used whose type of compression in SWs is already known. For example, different samples were studied by placing molybdenum or aluminium standards nearby, which were subjected to the action of SWs along with the samples of interest (the so-called loaded standard). This method is convenient because the position of the sample lines is determined in this case relative to the lines of the standard substance recorded in the same X-ray pattern [19, 27, 28]. In experiments performed in Refs [22, 29], the standard was not subjected to SW action, but its lines were also recorded on the same film with the sample lines (the unloaded standard).

Most of the PXRD papers are devoted to the study of single crystals. A *lithium fluoride* (LiF) crystal has been investigated most thoroughly. This cubic NaCl type crystal without high-pressure phase transitions is used in pulsed X-ray diffraction studies more often than other crystals because its compressibility in SWs has been investigated in detail by other methods. Nevertheless, to date the behavior of LiF is not completely clear.

At pressures of 6.6 and 13.5 GPa, L A Egorov and coauthors observed reflections corresponding to the isotropic compression of the lattice of LiF single crystals with the (100), (110), and (111) crystallographic planes oriented perpendicular to the SW direction [22]. At the same time, the X-ray patterns exhibited diffraction lines coinciding with the lines of the uncompressed crystal. The authors assigned them to the compressed crystal regions, but turned and compressed along the $\langle 111 \rangle$ direction. In this case, the volume compressibility $\sigma = V_0/V$ of crystal regions compressed isotropically and crystal regions compressed along the $\langle 111 \rangle$ direction was the same, equal to the compressibility calculated from the shock adiabat:

$$\sigma = \frac{D}{D-u}\,,$$

where D and u are the shock wave and particle velocities, respectively. This interpretation of unshifted lines in X-ray patterns seems controversial at present; however, such lines were also observed in studies of other substances [22, 29].

At pressures up to 5 GPa, a different compressibility was observed for LIF single crystals with various orientations. Crystals with the (100) orientation were compressed both in the SW propagation direction and perpendicular to it, whereas crystals with the (111) orientation did not show the transverse compressibility [15].

At pressures of 22 and 24 GPa, K Kondo and coauthors also found the absence of the isotropic compression of the LiF crystal lattice. In this case, the lattice compressibility in the $\langle 100 \rangle$ direction was greater than the compressibility that would be observed in the case of isotropic deformation, while the compressibility in the $\langle 111 \rangle$ direction was smaller. The anisotropic compression was also revealed in the studies of an LiF polycrystal at $P = 18$ GPa [9, 11]. At higher pressures of 30 GPa [5], 38.5 GPa [30], and 40–110 GPa [24], only the isotropic compression of the crystal lattice was observed.

The deformation pattern for *sodium chloride* (NaCl) crystals is different. The one-dimensional deformation of the lattice was observed in the [100] direction at pressures of 0.3–1 GPa [7], 1.75 GPa [13], and 30 GPa [12]. Due to a short exposure time (4 ns), the authors of Ref. [12] managed to record the SW structure (elastic and plastic waves) by taking photographs at different moments after the arrival of the SW on the sample surface.

In a *potassium chloride* (KCl) single crystal, the isotropic compression of the lattice in the $\langle 100 \rangle$ direction was observed at pressures lower than the phase transition pressure of 1.4–2 GPa.

In polycrystalline *aluminium* at low pressures (1.92, 2.97, and 3.91 GPa), the lattice compression close to uniaxial was observed from the (111) and (200) diffraction lines. At higher pressures of 11.8 and 23.1 GPa, the (111) and (200) diffraction lines were also obtained in work [18], but changes in the Al lattice parameter calculated from these lines proved to be different. While the compressibility calculated from the shift of the (200) line, assuming that the lattice symmetry is preserved, proved to be equal within the scatter of the measurement to the bulk compressibility (obtained from the shock adiabat), the compressibility calculated from the shift of the (111) line proved to be 1.03–1.04 times greater than the bulk compressibility. This suggests that the deformation of the cubic Al crystal lattice is anisotropic along crystallographic axes. Photographs of the Al single crystal oriented in the $\langle 111 \rangle$ direction at a pressure of 32 GPa demonstrated isotropic compression [6].

The behavior of *beryllium* was studied in Ref. [22]. At a pressure of 22.8 GPa, an X-ray pattern with the (100) and (101) lines was obtained. It was concluded from the X-ray diffraction data that the hexagonal Be lattice is compressed along the crystallographic c-axis.

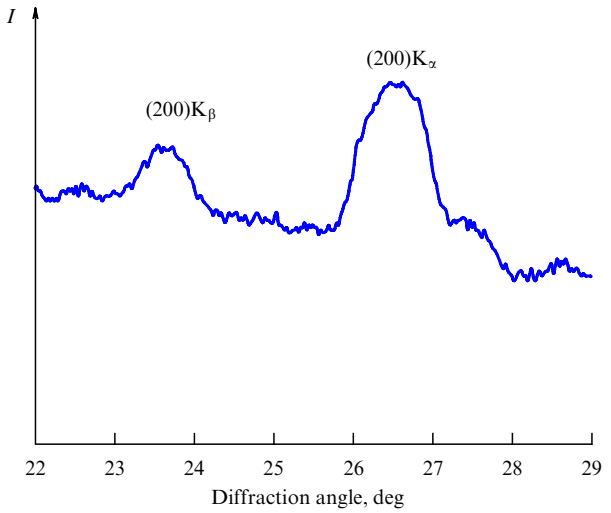

Figure 2. X-ray pattern of molybdenum in an SW at $P = 15$ GPa.

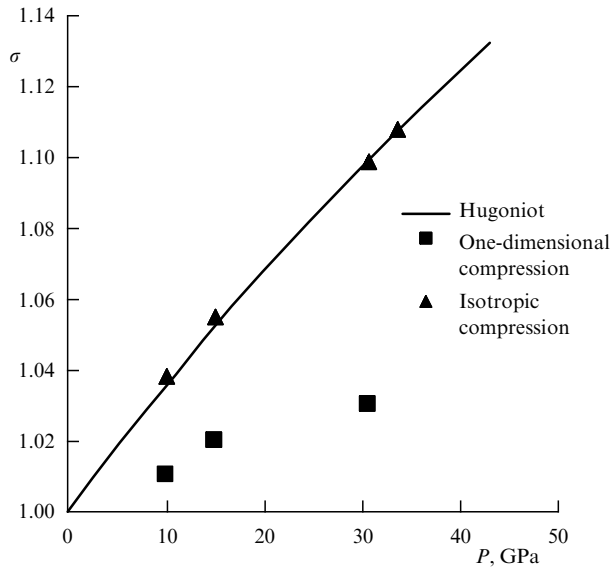

Figure 3. Shock compressibility of molybdenum. The Hugoniot [32] compared with compression calculated from X-ray diffraction data, assuming the isotropic and uniaxial deformations of the polycrystal lattice.

Another example of studying the type of compression of a material undergoing no phase transformations is the investigation of polycrystalline textured *molybdenum* [19]. Experiments were performed at pressures of 10, 15, 30.5, and 33.5 GPa. Figure 2 shows the X-ray pattern for Mo at $P = 15$ GPa. Two diffraction (200) lines from the K_α and K_β lines of a molybdenum anode were recorded. The spacing d of lattice planes was determined from the angular distance between the K_α and K_β lines. The accuracy of measuring d by this method is low because the compressibility of Mo in this pressure range is small, and therefore an increase in the angular distance between the lines is insignificant. According to estimates, the accuracy of measuring d reaches 0.001 nm, and of σ 2–3%. The results are displayed in Fig. 3, where the values of σ calculated assuming that compression is isotropic and uniaxial (in the SW propagation direction) are presented. These data suggest that within the accuracy achieved isotropic compression is observed behind the SW front in molybdenum for 200–300-ns X-ray pulses in the pressure interval studied.

All the studies of *silicon* single crystals performed by different researchers demonstrated uniaxial compression at pressures below the phase transition pressure [14, 33, 34] (the transition onset in an SW was revealed in the region of 12–13 GPa). This behavior of Si was explained by the low velocity and density of dislocations [14]; in this case, deformation has no time to relax plastically during photographic process and the lattice compression remains uniaxial.

The data obtained upon the compression of a *copper* single crystal along the ⟨100⟩ direction at $P = 18$ GPa are assigned either to isotropic hydrostatic compression [14] or to a deviation from hydrostatics [35]. According to the estimates of the authors, the dislocation structure in the case of copper, unlike that in Si, allows plastic deformation to proceed for times shorter than a microsecond.

Finally, the uniaxial compression of an *iron* lattice in the ⟨100⟩ direction at a pressure of 5.4 GPa was observed in Ref. [36].

Thus, we considered the results of structural studies of materials without phase transitions in SWs (or in the states below these transitions if the latter are present in these materials). The aim of these studies was to elucidate the type of compressibility at the crystal lattice level. In this regard, we paid attention mainly to final conclusions, by omitting the details of experiments, although some of them are quite significant, for example, the X-ray exposure time, the lifetime of the state under study, and the relation between these two times. Materials that have been studied differ in their crystal lattices (cubic or hexagonal) and chemical bonds (metals, halides, etc.), and they all can have their own kinetic parameters of the structural relaxation and deformation mechanisms requiring further investigations. Obviously, it is promising to use the concepts of the dislocation structure and microscopic mechanisms of the plastic flow to analyze the X-ray diffraction data.

Below, we consider the results of studies concerning the changes in the structure of materials during SW-driven phase transitions.

The first such study was reported in Ref. [5], where the X-ray patterns of shock-compressed pyrolytic *boron nitride* (BN) were obtained. Single-crystal samples oriented by the (001) plane parallel to the shock front were utilized. The diffraction (001) line was also recorded in X-ray patterns. At pressures of 14.5 and 20.5 GPa, the decrease in the lattice parameter c was observed. At $P = 24.5$ GPa, a line with $d = 0.220$ nm appeared in the X-ray pattern This line was interpreted by the authors as the (100) reflection of the wurtzite-like phase.

Graphite was studied in Ref. [4]. The change in the lattice parameter, $c/c_0 = 0.82$, was measured from the shift of the (002) line during SW loading (pressure was not indicated). By assuming that $a/a_0 = 0.99$, the authors obtained $\sigma = 1.25$, in accordance with the value obtained from the Hugoniot in the hydrostatic approximation.

To confirm the assumption about the difference in the compressibilities along the ⟨100⟩ and ⟨001⟩ directions, it was necessary to measure the pressure dependences of both the parameters of the hexagonal graphite lattice. This was done in Ref. [28] for natural graphite samples. The compressibility along the basic c-axis was determined from the angular shift of the (002) line, and along the a-axis from the shift of the

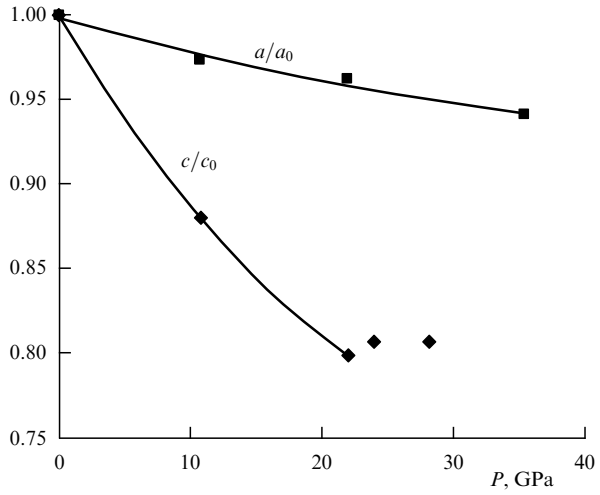

Figure 4. Pressure dependences of the relative change in the parameters of a graphite lattice in an SW (c/c_0 — rhombs, and a/a_0 — squares).

(110) line. Because X-ray patterns should have the required intensity, different lines were obtained from samples with various textures and differing initial densities [the (002) and (100) lines were obtained from samples with $\rho_0 = 2.15$ and 1.93 g cm^{-3}, respectively]. The estimates made by the authors showed that this did not introduce a large error into the interpretation of the results. Experiments were performed at pressures of 11, 22, 24, 28, and 35.5 GPa. The results are presented in Fig. 4. The analysis of these results leads to the following conclusions:

(1) The shock compressibility of graphite along the $\langle 001 \rangle$ c-axis is greater than that along the $\langle 100 \rangle$ a-axis.

(2) The values of the volume compressibility calculated from X-ray diffraction data at pressures of up to 22 GPa are in good agreement with those obtained from the Hugoniot in the hydrodynamic approximation.

(3) The break in the plot of c/c_0 at $P \approx 22$ GPa indicates the phase transformation. It is impossible to calculate compressibility from X-ray diffraction data at pressures above this value because, along with graphite, a new high-pressure phase is already present behind the SW front.

The high-pressure phase was detected in the X-ray pattern of graphite at a pressure of 35.5 GPa, when, during the photographing of the (002) line, a line with $d = 0.218$ nm was recorded, which was interpreted as the (100) line of hexagonal diamond — lonsdaleite.

Potassium chloride (KCl) single crystals were investigated at pressures exceeding the phase transition pressure in the range from 2 to 6 GPa [22, 31, 37]. In all cases, the authors observed reflections from the high-pressure phase. The transition of KCl from the NaCl type structure to the CsCl structure, which is known from static experiments, occurs at a pressure of ~ 2 GPa. The phase transition onset in dynamics was revealed at the same pressure [38]. The authors of all three papers observed, along with lines belonging to the CsCl type structure, diffraction lines that could not be interpreted within the framework of the two known phases, and were assigned to intermediate states accompanying the phase transformation process. However, the intermediate structures were interpreted by the authors differently. A whole package of rhombohedral structures was described in Ref. [22], which were produced depending on the loading pressure on a sample and its orientation with

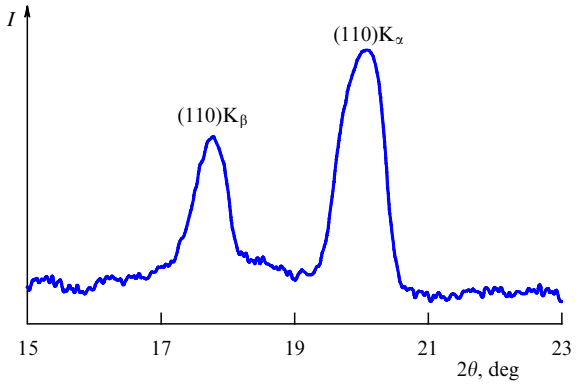

Figure 5. X-ray pattern of siliceous iron in an SW at $P = 10$ GPa.

respect to crystallographic axes. In paper [37], the intermediate structure at $P = 3$ GPa was identified as a simple cubic structure.

The X-ray patterns of the high-pressure ε-phase of *iron* were obtained by applying PXRD analysis in Ref. [19]. The intensity of pulsed X-ray patterns was increased by employing the textured samples of Fe + 3% Si transformer steel with a density of 7.68 g cm^{-3} and the $\langle 100 \rangle \{110\}$ texture increasing the (100) diffraction line intensity in X-ray patterns. It is known that a Fe–Si alloy, like pure iron, undergoes the $\alpha \rightarrow \varepsilon$ phase transition in SWs (the transition onset is at 12–15 GPa) [39]. The X-ray patterns of siliceous Fe were obtained at pressures of 10, 15, and 29 GPa. Figure 5 displays the X-ray pattern photographed at $P = 10$ GPa.

As would be expected, only the (110) K_α and K_β lines of the α-phase are observed in the preliminary and explosion X-ray patterns at pressures below the phase transition pressure. At pressures of 15 and 20 GPa, the pattern changes (Fig. 6): the diffraction lines in X-ray patterns correspond to the ε-phase.[1] The crystallographic data for this phase are given in Table 1.

Table 1. Crystallographic data for the ε-phase of Fe.

Parameter	$P = 15$ GPa	$P = 29$ GPa
d (100), nm	0.220	0.215
d (002), nm	0.204	0.201
d (101), nm	0.191	0.188
a, nm	0.252	0.247
c, nm	0.408	0.401
a/c	1.62	1.62

An attempt was made to study the phase transformation in *zirconium* [27]. As the static pressure is increased, Zr undergoes a transition from the hexagonal closely packed modification (the α-phase) to the hexagonal ω-phase. The

[1] The statement of the authors of papers [36] and [40] that they were the first to obtain *in situ* X-ray patterns of SW compressed iron is not correct. The X-ray patterns of Fe in SWs were first obtained by A M Podurets, A I Barenboim, V V Pul, and R F Trunin at VNIIEF in 1986–1987. The first results were published in "Proceedings of the IV-th All-Union Conference on Detonation" [41] in 1988, and in a Russian academic journal in 1989 [19]. The results of Fe studies were also published in English in "Proceedings of the International Conference on Condensed Matter under High Pressures" in Bombay in 1996 [42].

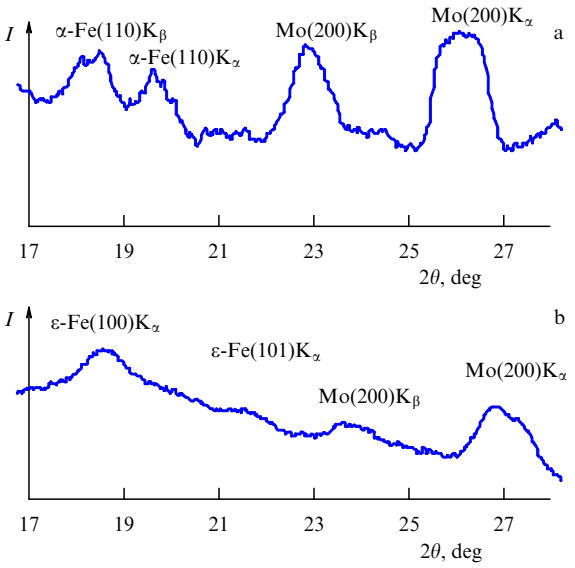

Figure 6. X-ray pattern of siliceous iron with a molybdenum standard in an SW (a) at $P = 0$ (preliminary photograph), and (b) at $P = 15$ GPa.

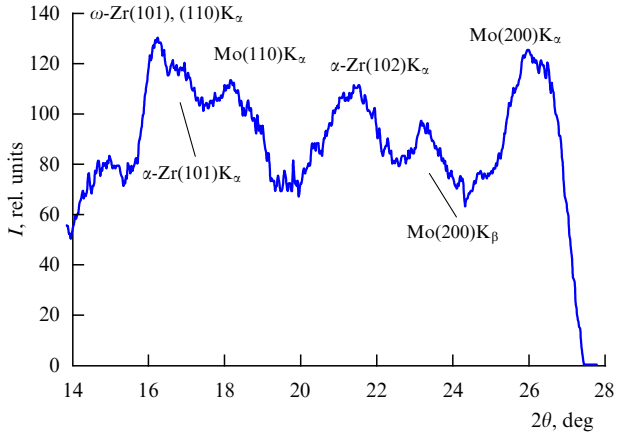

Figure 7. X-ray pattern of zirconium with a molybdenum standard unloaded after compression in an SW of up to $P = 12$ GPa.

phase transformation in Zr also occurs upon shock loading. The break in the Hugoniot was revealed at $P = 26$ GPa [43]. It is not clear so far to which transformation this break corresponds because, as a rule, pressures at which transitions occur at static and dynamic loadings are close. In contrast, phase transformations in Zr in shock waves occur at pressures considerably exceeding the equilibrium pressure. However, despite numerous experimental data, the crystallographic nature of the phase transformation (or transformations) in Zr remains unclear.

The X-ray patterns of Zr samples loaded with shock waves were photographed at pressures of 5, 9.5, 15, and 25 GPa. At pressures of 5 and 9.5 GPa, the structure of the initial α-phase was observed. At higher pressures, the picture changed. At $P = 15$ GPa, the two Zr lines corresponding to the interplanar spacings of 0.227 and 0.211 nm were detected in X-ray patterns. The line with $d = 0.211$ nm was also observed at $P = 29$ GPa. It is impossible to relate unambiguously these interplanar spacings to the structure of an isotropically compressed ω-phase (or the β-phase of Zr). We can only assume that either one of these highly deformed phases exists behind the SW front or some different Zr phase is produced. Because both these unidentified lines can belong to different phases with various degrees of deformation, it is impossible to assign them unambiguously.

It is known from experiments with the recovery of shock-loaded samples that the ω-phase in the pressure interval 9–24 GPa is recovered after unloading [44]. To 'match' the data obtained by the method of pulsed X-ray photography at the moment of loading with the data obtained for recovered samples, experiments were performed in which the X-ray pattern of the free surface of a Zr sample was captured after an SW at a pressure of 12 GPa arrived at this surface and the unloading started.

The X-ray pattern obtained (Fig. 7) shows that within 1 μs after the SW emergence on the sample surface, the sample consisted of a mixture of the α- and ω-phases, which confirms the data obtained in the study of recovered samples. The X-ray patterns did not contain the lines of an unknown nature.

A complex sequence of structural transformations in an SW was detected in *bismuth*. At the lowest pressure of 6.7 GPa, the Bi-V structure revealed itself [27], which is known from static measurements. A pressure of 6.7 GPa lies near the stability region of this phase. The phase VI region, which has the body-centered cubic (bcc) structure lies at higher pressures.

At pressures of 8.5 and 13.7 GPa, the X-ray pattern was the same and contained a diffraction line corresponding to the interplanar spacing of 0.222–0.225 nm. Such spacings could belong to the (111) line of the cubic structure; however, a line with such indices is forbidden in a bcc lattice due to extinction effect (caused by the structure symmetry). If we assume that the bcc-phase structure behind the SW front in Bi differs from ideally symmetric, then no extinction of this line will occur. The Bi structure at pressures of 8.5 and 13.7 GPa was interpreted as the distorted bcc structure, which was not observed under static conditions. This conclusion is confirmed by the presence of lines with $d = 0.185-0.202$ nm in some X-ray patterns, which can correspond to the (200) line of the bcc phase; at $P = 9$ GPa, the value of d for this phase under static conditions was 0.1900 nm [45].

At a pressure of 22 GPa, a broad diffuse halo revealed itself in X-ray patterns in the region of angles θ corresponding to the interplanar spacings from 0.25 to 0.3 nm (Fig. 8). The diffuse halo in the absence of distinct diffraction peaks suggests that the long-range order in the crystal is violated, and the structure becomes closer to the structure of liquids or amorphous matter.

At a pressure of 27 GPa, no diffraction lines were detected in any explosion X-ray patterns. This can be explained by the melting of Bi in the SW. The pressure in these experiments is rather close to the melting threshold of Bi, equal to 33 GPa, which was obtained by another experimental technique [46].

Thus, the sequence of structural changes in Bi in the SW at the pressures considered above demonstrates considerable differences between the SW picture and the static picture. Amorphization observed at $P = 22$ GPa suggests that a further increase in pressure will lead to melting, i.e., structure disturbance preceding the complete loss of the long-range order.

We have analyzed the main results obtained by the pulsed X-ray diffraction method, not considering thoroughly the technical details. However, it is the technical aspects of the

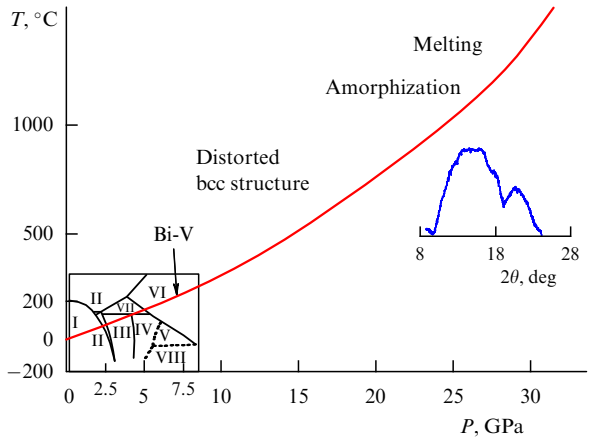

Figure 8. Sequence of structural changes in bismuth in an SW. The solid curve depicts a Hugoniot. The inset to the figure at the left corner shows the static phase diagram of Bi [38]; the inset at the right displays the X-ray pattern of amorphous Bi.

method that play a key role in its further development. The examples considered in the paper show that the PXRD analysis can be very informative and useful for the understanding of processes proceeding upon the action of SWs on a material. Therefore, this method will be undoubtedly further used and developed. Notably, to obtain more reliable data, it is necessary to employ more stable loading systems and radiation sources. However, difficulties encountered in the use of the PXRD analysis do not concern the experimental equipment alone. The experimental data accumulated at present demonstrate the complexity of processes accompanying the shock loading of crystals. It is necessary to develop the microstructure concepts of the shock compression, mechanism, and kinetics of phase SW transformations. Therefore, PXRD experiments should not only demonstrate the phenomenon (today the illustrative type of experiment is often due to their comparatively low accuracy, which is not discussed here), but also facilitate the understanding of the physical mechanism of the phenomenon. In particular, PXRD analysis can be useful in studying melting in SWs, which was demonstrated for bismuth.

The author is grateful to R F Trunin for many helpful discussions and scientific editing of the paper and his attention for many years to PXRD method at RFNC–VNIIEF.

References

1. Al'tshuler L V et al. in *Devyatoe Nauchno-Tekhnicheskoe Soveshchanie po Primeneniyu Rentgenovskikh Luchei k Issledovaniyu Materialov, 18–24 Dekabrya 1967 g., Leningrad, Tezisy Dokladov* (9th Scientific and Technical Meeting on X-Ray Applications for Studying Materials, 18–24 December 1967, Leningrad, Abstracts of Papers) (Leningrad, 1967) p. 37
2. Egorov L A et al. *Prib. Tekh. Eksp.* (2) 200 (1968)
3. Egorov L A, Nitochkina E V, Orekin Yu K *Pis'ma Zh. Eksp. Teor. Fiz.* **16** 8 (1972) [*Sov. Phys. JETP* **16** 4 (1972)]
4. Johnson Q et al. *Phys. Rev. Lett.* **25** 1099 (1970)
5. Johnson Q, Mitchell A C *Phys. Rev. Lett.* **29** 1369 (1972)
6. Johnson Q, Mitchell A C, Evans L *Appl. Phys. Lett.* **21** 29 (1972)
7. Jamet F, in *High Pressure Science and Technology, Proc. VII AIRAPT Conf., Le Creusot, 1978*, p. 974
8. Kondo K, Sawaoka A, Saito S, in *Proc. of the 4th Intern. Conf. on High Pressure, Kyoto, 1974*, p. 845
9. Kondo K, Sawaoka A, Saito S, in *High Velocity Deformation of Solids, Tokyo, 1978*, Vol. B, p. 176
10. Kondo K et al., in *High Pressure Science and Technology, New York, 1979*, Vol. 2, p. 883
11. Kondo K, Sawaoka A, Saito S, in *High Pressure Science and Technology, New York, 1979*, Vol. 2, p. 905
12. Muller F, Schulte E *Z. Naturforsch. A* **33** 918 (1978)
13. Zaretsky E, in *Shock Compression of Condensed Matter — 1997, Woodbury, 1998*, p. 883
14. Loveridge-Smith A et al. *Phys. Rev. Lett.* **86** 2349 (2001)
15. Rigg P A, Gupta Y M *Phys. Rev. B* **63** 094112 (2001)
16. Wark J S et al. *Phys. Rev. B* **35** 9391 (1987)
17. Wark J S et al. *J. Appl. Phys.* **68** 4531 (1990)
18. Al'tshuler L V et al. *Zh. Eksp. Teor. Fiz.* **81** 672 (1981) [*Sov. Phys. JETP* **54** 359 (1981)]
19. Podurets A M et al. *Izv. Akad. Nauk SSSR Fiz. Zemli* (6) 26 (1989)
20. Umanskii Ya S *Rentgenografiya Metallov i Poluprovodnikov* (X-radiography of Metals and Semiconductors) (Moscow: Metallurgiya, 1969) p. 209
21. Barenboim A I et al. *Prib. Tekh. Eksp.* (1) 189 (1992)
22. Egorov L A et al. *Zh. Eksp. Teor. Fiz.* **103** 135 (1993) [*JETP* **76** 73 (1993)]
23. Zaretskii E B et al. *Teplofiz. Vys. Temp.* **29** 1002 (1991)
24. Johnson Q, Mitchell A C, in *High Pressure Science and Technology. Proc. VII AIRAPT Conf., Le Creusot, 1978*, p. 977
25. Zaretsky E *J. Phys. IV France* **7** (C3) 329 (1997)
26. Woolsey N C et al., in *Shock Compression of Condensed Matter — 1995, Woodbury* Pt. 2 (New York: AIP Press, 1996) p. 997
27. Podurets A M, Dorokhin V V, Trunin R F *Teplofiz. Vys. Temp.* **41** 254 (2003) [*High Temp.* **41** 216 (2003)]
28. Podurets A M et al. *Izv. Akad. Nauk SSSR Fiz. Zemli* (1) 107 (1991)
29. Egorov L A et al. *Khim. Fiz.* **14** (2–3) 100 (1995)
30. Barenboim A I, Dorokhin V V, Egorov L A, in *1 Vsesoyuz. Simp. po Makroskopicheskoi Kinetike i Khimicheskoi Gazodinamike, Alma-Ata, Tezisy Dokladov* (1st All-Union Symp. on Macroscopic Kinetics and Chemical Hydrodynamics, Alma-Ata, Abstract of Papers) Vol. 2, Pt. 2 (Chernogolovka, 1984) p. 51
31. d'Almeida T, Gupta Y M *Phys. Rev. Lett.* **85** 330 (2000)
32. Trunin R F (Ed.) *Eksperimental'nye Dannye po Udarno-Volnovomu Szhatiyu i Adiabaticheskomu Rasshireniyu Kondensirovannykh Veshchestv* (Experimental Data on the Shock Compression and Adiabatic Expansion of Condensed Matter) (Sarov: RFYaTs–VNIIEF, 2006)
33. Podurets A M, Mokhova V V, in *8 Intern. Conf. on High Pressure Semiconductor Physics, August 9–13, 1998, Thessaloniki*
34. Kishimura H et al. *Phys. Rev. B* **74** 224301 (2006)
35. Meyers M A et al. *Acta Mater.* **51** 1211 (2003)
36. Kalantar D H et al. *Phys. Rev. Lett.* **95** 075502 (2005)
37. Zaretskii E B et al. *Dokl. Akad. Nauk SSSR* **316** 111 (1991) [*Sov. Phys. Dokl.* **36** 76 (1991)]
38. Tonkov E Yu *Fazovye Diagrammy Soedinenii pri Vysokom Davlenii* (Phase Diagrams of Compounds at High Pressure) (Moscow: Nauka, 1983)
39. Graham R A *J. Appl. Phys.* **39** 437 (1968)
40. Hawreliak J et al. *Phys. Rev. B* **74** 184107 (2006)
41. Podurets A M et al., in *IV Vsesoyuz. Konf. po Detonatsii, Telavi, 1988* (IVth All-Union Conference on Detonation, Telavi, 1988) Vol. 1, p. 162
42. Podurets A M, Barenboim A I, Trunin R F, in *Intern. Conf. on Condensed Matter Under High Pressures, Bombay, 1996, Proc.: Advances in High Pressure Research in Condensed Matter* (Eds S K Sikka, S C Gupta, B K Godwal) (New Delhi, 1997) p. 285
43. McQueen R G et al., in *High-Velocity Impact Phenomena* (Ed. R Kinslow) (New York: Academic Press, 1970) p. 293 [Translated into Russian (Moscow: Mir, 1973) p. 299]
44. Kutsar A R, Lyasotski I V, Podurets A M, Sanches-Bolinches A F *High Pressure Research* **4** 475 (1990)
45. Schaufelberger Ph, Merx H, Contre M *High Temp. High Pressures* **4** 111 (1972)
46. Trunin R F et al. *Teplofiz. Vys. Temp.* **33** 222 (1995)